

Syntheses, Crystal Structures, and Magnetic Properties of Copper(II) and Manganese(II) Compounds Constructed from 5-Sulfoisophthalic Acid (H₃SIP) and 2,2'-Bipyridine (bpy) Ligands

Qing-Yan Liu,^[a] Yu-Ling Wang,^[b] Jun Zhao,^[a] and Li Xu*^[a]

Keywords: Dinuclear copper / Manganese / Hydrothermal synthesis / Crystal structures / Magnetic properties

The compounds [Cu₂(SIP-O)(bpy)₂(H₂O)₂]·7H₂O (**1**) and [Mn(HSIP)(bpy)]_n (**2**) were synthesized by the hydrothermal reactions of Cu(OH)₂ or MnCl₂, 5-sulfoisophthalic acid monosodium salt (NaH₂SIP), and 2,2'-bipyridine (bpy). Single-crystal X-ray diffraction reveals that the unprecedented hydroxylation of SIP³⁻ catalyzed by Cu²⁺ occurs and produces the discrete SIP-O⁴⁻-bridged dicopper(II) compound **1**. The hydrogen-bonding association of the seven lattice water molecules of **1** leads to the formation of an unusual 2D-layer-

ered water consisting of fused four- and sixteen-membered water rings and a discrete water octamer consisting of a cyclic tetramer and four dangling water molecules. Compound **2** is a 3D coordination polymer and has two kinds of topologically equivalent 4-connected nodes based on Mn²⁺ and HSIP²⁻ with a rare (4.6⁵) topology.

(© Wiley-VCH Verlag GmbH & Co. KGaA, 69451 Weinheim, Germany, 2008)

Introduction

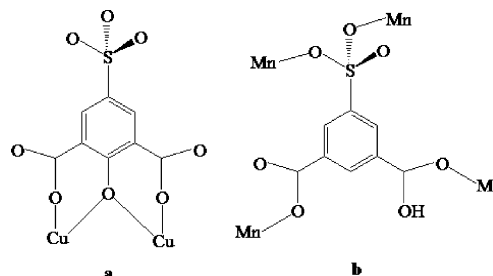
The design and construction of metal–organic frameworks (MOFs) is one of the most active areas of materials research in recent years. The intense interest in these materials is driven by their potential applications as functional materials (catalysis, magnetism, electric conductivity, and nonlinear optics) and intriguing structural diversities.^[1–3] Many efforts have thus far been devoted to the study of carboxylate-based compounds.^[4] However, relatively little attention has been paid to the sulfonate-based assemblies, despite the fact that the sulfonate group bears diversified coordinating modes and ligating sensitivity to the nature (hardness) of the metal ions.^[5] Recently, 5-sulfoisophthalic acid (H₃SIP) was successfully used to investigate the lanthanide contraction effect^[6] and the coordination polymer chemistry of the main group metal lead(II),^[7] because of its multiple coordinating modes and the sensitivity of the sulfonate group to the surrounding chemical environment. The present work deals with the hydrothermal reaction of Cu(OH)₂ (or MnCl₂), NaH₂SIP, and bpy at 160 °C, which produces the dimeric [Cu₂(SIP-O)(bpy)₂(H₂O)₂]·7H₂O (**1**) {or 3D [Mn(HSIP)(bpy)]_n (**2**)}. Unprecedented in situ hydroxylation of SIP occurs in the case of Cu(OH)₂. Mean-

while, the seven crystal lattice water molecules in **1** form an unprecedented 2D-layered water with 4.8² topology consisting of a 16-membered ring fused to a four-membered ring, and a discrete water octamer consisting of a cyclic tetramer and four dangling water molecules. Mn^{II} compound **2** has an interesting 3D structure pillared by sulfonate groups, and it has a unique (4.6⁵) topology based on two equivalent 4-connected nodes.

Results and Discussion

Hydrothermal Synthesis

Hydrothermal synthesis is widely employed to produce new materials with diverse structural architectures, but it remains a black box. This method can minimize the problems associated with ligand solubility and enhance the reactivity of reactants in favor of efficient molecular building during the crystallization process. In the preparation of compounds **1** and **2** (Scheme 1), the reaction conditions are



Scheme 1. Coordination modes of the SIP-O and HSIP ligands observed in compounds **1** and **2**.

[a] State Key Laboratory of Structural Chemistry, Fujian Institute of Research on the Structure of Matter, Chinese Academy of Sciences, Fuzhou, Fujian, 350002, P. R. China
Fax: +86-591-83705045
E-mail: xli@fjirsm.ac.cn

[b] College of Chemistry and Chemical Engineering, Jiangxi Normal University, Nanchang, Jiangxi 330022, P. R. China

almost the same but the outcomes are quite different. The solution reactions between Cu^{II} and SIP were reported previously to produce Cu^{II} –SIP coordination polymers.^[5] Under the present hydrothermal conditions, however, the unusual hydroxylation of SIP occurs in situ to yield the organic compound 2-oxo-5-sulfoisophthalic acid (SIP-O^+), which is indicative of the catalytic oxidation properties of Cu^{2+} ions at elevated temperatures. The similar in situ metal/ligand redox reaction with isophthalic acid was reported previously.^[8]

Crystal Structure of $[\text{Cu}_2(\text{SIP-O})(\text{bpy})_2(\text{H}_2\text{O})_2] \cdot 7(\text{H}_2\text{O})$ (1)

X-ray structural analysis clearly reveals the existence of an additional oxygen atom attached to SIP to form SIP-O^+ , which achieves the charge balance. The structure of the host $[\text{Cu}_2(\text{SIP-O})(\text{bpy})_2(\text{H}_2\text{O})_2]$ motif is shown in Figure 1, wherein the two crystallographically independent but geometrically similar Cu^{II} atoms are bridged by two unidentate carboxylate groups and one bridging phenyl oxygen atom (O6). One bpy ligand and one water oxygen atom complete a distorted square-pyramidal coordination geometry of each Cu center. The Cu–O bond lengths range from 1.902(3) to 2.197(4) Å, and the Cu–N bond lengths vary from 1.978(3) to 2.007(3) Å (Table 1). The bond dimensions involving Cu are normal, and they are comparable to the values in related copper(II) complexes.^[5,9] The dinuclear copper units are interconnected through the hydrogen bonds between the coordinating water molecules and the carboxylate groups [$\text{O} \cdots \text{O} = 2.938(5)$ and $2.856(5)$ Å] into a 1D chain parallel to the *c* axis (Figure 2a and Table 2). The adjacent chains are linked together through hydrogen bonds [$\text{O} \cdots \text{O} = 2.800(7)$ and $2.814(7)$ Å] between the sulfonate groups and the two lattice water molecules (O6W and O7W) to form a 2D supramolecular layer in the *bc* plane (Figure 2b).

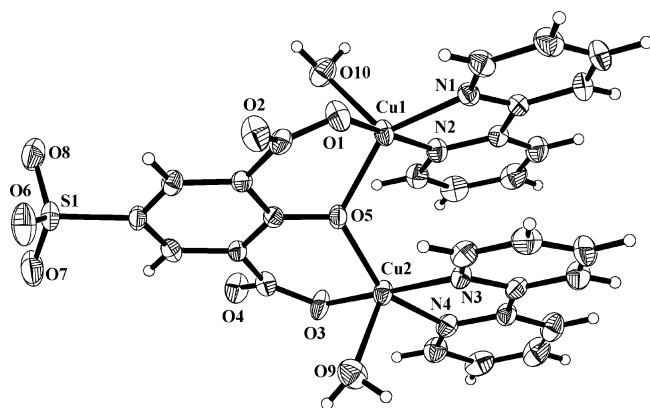


Figure 1. ORTEP drawing of $[\text{Cu}_2(\text{SIP-O})(\text{bpy})_2(\text{H}_2\text{O})_2]$ with 30% probability thermal ellipsoids.

The hydrogen-bonding association of four of the seven lattice water molecules leads to the formation of a 2D-layered water consisting of fused four- and sixteen-membered water rings (Figure 3). The geometrical parameters of the water clusters are summarized in Table 2. The centrosym-

Table 1. Selected bond lengths [Å] and bond angles [°] for **1** and **2**.^[a]

Compound 1			
Cu1–O1	1.902(3)	O10–Cu1–N2	92.35(14)
Cu1–O5	1.998(3)	O5–Cu1–O1	88.66(12)
Cu1–N1	1.990(3)	O5–Cu1–N2	93.37(13)
Cu1–N2	1.978(3)	N1–Cu1–N2	81.20(14)
Cu1–O10	2.172(3)	N1–Cu1–O1	92.76(13)
Cu2–O3	1.905(3)	O9–Cu2–O3	95.06(14)
Cu2–O5	1.958(3)	O9–Cu2–O5	105.52(13)
Cu2–N3	1.982(3)	O9–Cu2–N3	90.73(14)
Cu2–N4	2.007(3)	O9–Cu2–N4	107.29(14)
Cu2–O9	2.197(4)	O5–Cu2–O3	89.77(12)
O10–Cu1–O1	94.13(14)	O5–Cu2–N3	93.18(13)
O10–Cu1–O5	101.59(13)	N4–Cu2–N3	81.49(14)
O1–Cu1–N1	117.57(14)	N4–Cu2–O3	92.31(13)
Compound 2			
Mn1–O5	2.192(3)	Mn1–O1A	2.156(3)
Mn1–O3C	2.149(3)	Mn1–O6B	2.185(3)
Mn1–N1	2.278(4)	Mn1–N2	2.272(4)
O3C–Mn1–O1A	105.76(13)	O1A–Mn1–N2	86.11(14)
O3C–Mn1–N1	96.29(15)	N1–Mn1–N2	71.81(15)
O5–Mn1–O6B	173.39(13)	O5–Mn1–O1A	93.74(13)
O5–Mn1–O3C	88.51(14)	O5–Mn1–N1	88.77(14)
O5–Mn1–N2	92.14(15)	O6B–Mn1–N1	88.38(15)
O6B–Mn1–N2	92.64(15)	O6B–Mn1–O1A	91.14(14)
O6B–Mn1–O3C	85.87(14)		

[a] Symmetry transformation for equivalent atoms: Compound 2: A: $x - 1/2, -y + 2/3, -z$; B: $-x + 1/2, y - 1/2, z$; C: $x, -y + 3/2, z - 1/2$.

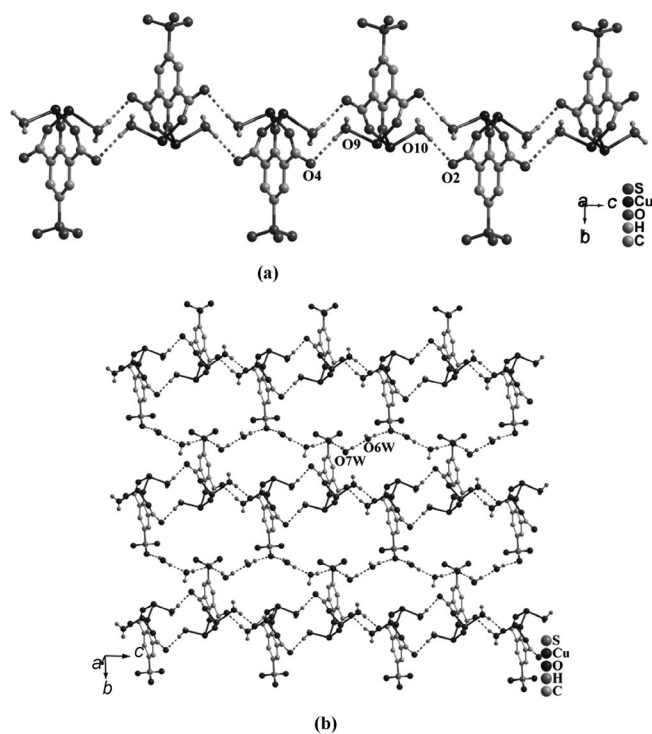


Figure 2. (a) 1D Hydrogen-bonded chain, (b) 2D hydrogen-bonded layer parallel to the *bc* plane (bpy has been omitted for clarity).

metric 16-membered water ring formed by O3W, O5W, O6W, O7W, and their equivalents are illustrated in Figure 3a with the dimension of approximately 9×10 Å, which

Table 2. Hydrogen bonds parameters in compound **1**.^[a]

D–H...A	D–H [Å]	H...A [Å]	∠DHA [°]	D...A [Å]
O1W–H1WA...O2WA	0.90(2)	2.02(2)	176(7)	2.918(7)
O1W–H1WB...O2W	0.89(2)	1.93(5)	178(9)	2.827(7)
O3W–H3WB...O5WB	0.93(6)	1.96(4)	156(8)	2.824(8)
O4W–H4WB...O1WA	0.92(9)	2.09(9)	166(1)	2.981(8)
O5W–H5WA...O3W	0.91(5)	1.92(4)	167(5)	2.805(7)
O5W–H5WB...O7WB	0.89(5)	1.82(3)	169(6)	2.706(7)
O6W–H6WB...O3W	0.95(2)	1.74(2)	168(6)	2.678(8)
O7W–H7WA...O6WC	0.89(4)	1.83(2)	172(5)	2.714(8)
O9–H9C...O5W	0.89(2)	1.86(2)	170(5)	2.736(6)
O10–H10B...O1W	0.88(2)	1.92(2)	168(5)	2.781(5)
O9–H9B...O4C	0.88(5)	2.06(5)	170(6)	2.938(5)
O10–H10C...O2D	0.88(4)	2.00(2)	166(4)	2.856(5)
O2W–H2WA...O8A	0.89(2)	1.98(3)	157(5)	2.823(6)
O2W–H2WB...O2	0.90(2)	2.25(11)	143(15)	3.014(6)
O3W–H3WA...O4	0.92(5)	1.85(3)	168(8)	2.759(6)
O4W–H4WA...O6	0.90(2)	2.08(3)	155(5)	2.919(7)
O6W–H6WA...O7B	0.91(2)	1.91(6)	168(0)	2.800(7)
O7W–H7WB...O7B	0.90(5)	1.96(3)	158(6)	2.814(7)

[a] Symmetry transformations used to generate equivalent atoms: A: $-x, -y + 1, -z$; B: $-x + 1, -y + 1, -z$; C: $x, -y + 1/2, z - 1/2$; D: $x, -y + 1/2, z + 1/2$.

represents a unique cyclic (H₂O)₁₆. A discrete acyclic (H₂O)₁₆ cluster, however is known.^[10] Theoretical calculations proposed five lowest energy (H₂O)₁₆ clusters, and the most stable one is the linear fused cube derived from the *D*_{2d} and *S*₄ forms of (H₂O)₈.^[11] However, its existence is not confirmed experimentally to date. Thus, our observation of the cyclic sixteen-membered ring in the 2D-layered water may be attributed to its different modes of connectivity with the surrounding water molecules and the interactions with the dinuclear copper motifs. As depicted in Figure 3b, O3W and O5W are hydrogen bonded to their symmetry-related equivalents to form a *D*_{2h}-symmetric cyclic water tetramer. Within the tetramer, the four water oxygen atoms are completely coplanar, and each water monomer acts as both a single hydrogen-bond donor and a single hydrogen-bond acceptor. The remaining hydrogen atoms are alternatively oriented above or below the ring plane to achieve the minimum H–H repulsion. In the 2D water sheet, the O...O separations range from 2.678(8) to 2.824(8) Å with an average distance of 2.745 Å, which is close to the corresponding value of 2.748 Å in the 2D supramolecular ice-like layer containing (H₂O)₁₂ rings in the organic compound bpedo·5H₂O [bpedo = *trans*-bis(4-pyridyl)ethylene dioxide].^[12] Moreover, the average O...O...O angle of 110.7° is similar to the tetrahedral geometry. From a topology viewpoint, the hydrogen-bonded 2D water layer can be regarded to have 4.8² topology (Figure 3c). This type of net, predicted by Wells^[13] but commonly observed for coordination frameworks^[14] and not previously observed for the water cluster, consists of three-connected nodes (O3W and O5W) shared by one tetragonal square unit (cyclic water tetramer) and two octagons (cyclic water hexadecamer). This type of water layer, to the best of our knowledge, is unprecedented. Additional O9–H9C...O5W hydrogen bonds anchor the 2D water layer to the host metal–organic supramolecular layer.

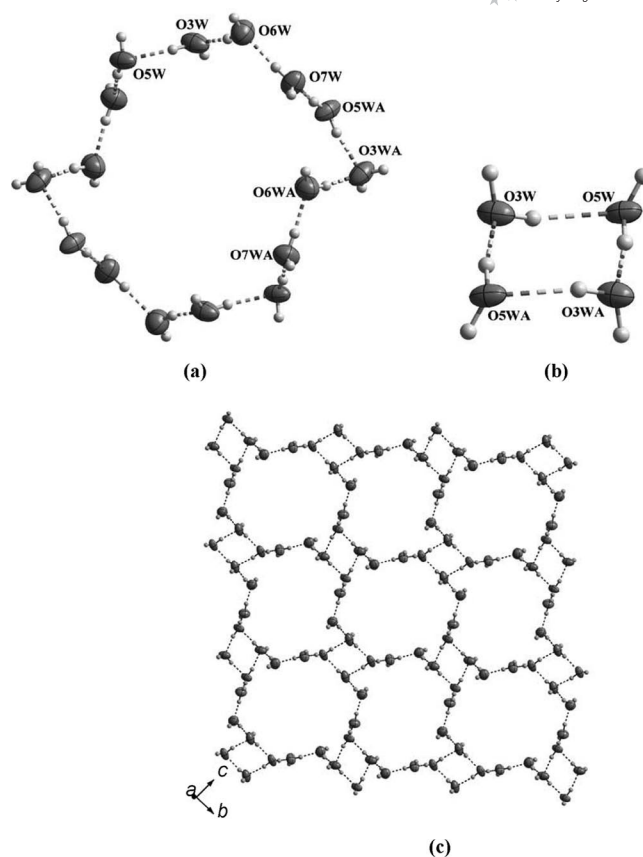


Figure 3. (a) The centrosymmetric (H₂O)₁₆ water ring; (b) the *D*_{2h}-symmetric cyclic water tetramer cluster in **1**; (c) view of the 2D water layer with 4.8² topology parallel to the *bc* plane.

The remaining three lattice water molecules (O1W, O2W, O4W) and one coordinating water molecule (O10) form the discrete water octamer consisting of cyclic tetramer and four dangling water molecules (Figure 4). This water octamer and the above-described 2D water layers are alternatively placed between the host supramolecular layers. In the centrosymmetric cyclic water tetramer formed by O1W and O2W and their equivalents, O1W acts as a hydrogen-bond donor and O2W as an acceptor. This type of cyclic (H₂O)₄ cluster is different from the one in the above-mentioned 2D water layer, but similar to that in the solid state complex {[Cd(dpp)(SIP)(H₂O)₃]+0.5Cd(H₂O)₆·5H₂O}_n [dpp = 1,3-bis(4-pyridyl)propane].^[15] This unusual conformation is be-

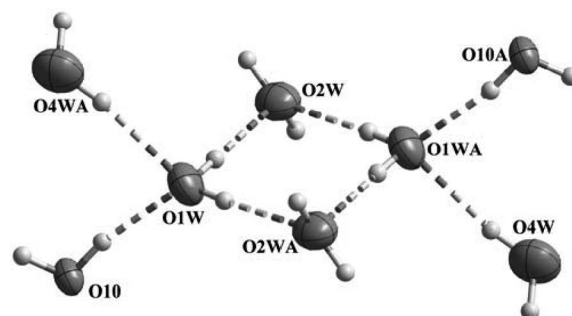


Figure 4. The centrosymmetric water octamer in **1**.

lied to result from the fact that the two water molecules (O4W and O10) both act as single hydrogen donors in the hydrogen bonds to O1W in the resulting centrosymmetric $(\text{H}_2\text{O})_8$ cluster. The common patterns for the water octamer experimentally found are cubane,^[16] opened cube,^[17] and cyclic ring.^[18] Theoretical calculations show that the cubane-like conformation with S_4 symmetry has an energy minimum, and it has been observed experimentally.^[16,19] Interestingly, the centrosymmetric $(\text{H}_2\text{O})_8$ cluster observed here is quite different from those theoretically predicted or experimentally found, which indicates that the conformation of water clusters varies with the host environment. The averaged $\text{O}\cdots\text{O}$ separation of 2.877 Å is slightly longer than the value of 2.745 Å in the cyclic $(\text{H}_2\text{O})_8$ cluster in the organic calix[4]resorcinarene supramolecular complex,^[18] 2.846 Å in the cubane water octamer,^[16] and 2.85 Å in the

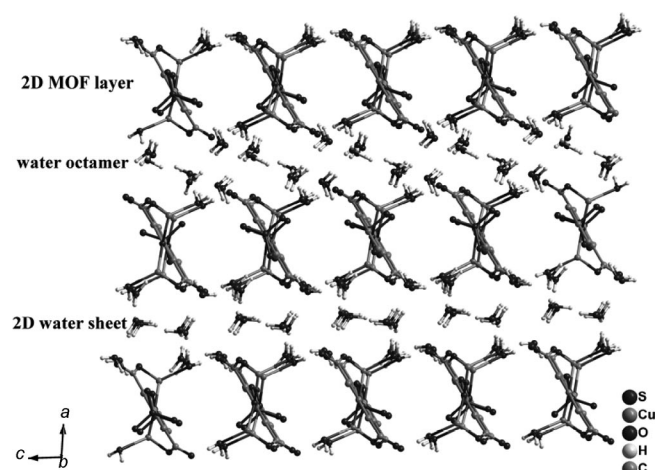


Figure 5. The hydrogen-bonded 3D supramolecular framework of **1**.

water octamer consisting of a cyclic water hexamer and two dangling water molecules.^[20] The remaining six hydrogen atoms per $(\text{H}_2\text{O})_8$ cluster unit are bonded to the carboxylate oxygen atoms and sulfonate oxygen atoms of the SIP-O ligand to form a 3D supramolecular network (Figure 5). Thus, the 2D-layered water and discrete water octamers occupy the voids between the layers and act as “glue” to assemble the dinuclear coordination units around them to give a 3D structure.

Crystal Structure of $[\text{Mn}(\text{HSIP})(\text{bpy})]_n$ (**2**)

The asymmetric unit in compound **2** consists of one manganese(II) ion, one HSIP dianion, and one bpy molecule. As depicted in Figure 6, the four equatorial positions of Mn^{2+} are occupied by two carboxylate oxygen atoms from two HSIP²⁻ ligands and one chelating bpy nitrogen atom; the benzene and bpy moieties are almost coplanar. Two sulfonate oxygen atoms from two HSIP²⁻ ligands take up the apical positions to complete the octahedral coordination geometry, and the O6B-Mn1-O5 angle is 173.3(1)°. The Mn–O bond lengths range from 2.152(3) to 2.192(2) Å, and the Mn–N bond lengths are 2.270(3) and 2.273(3) Å, which are comparable with the values in related Mn(II) complexes.^[21] The HSIP²⁻ ligand adopts a tetradentate bridging coordination mode through its monodentate carboxylate groups and bidentate sulfonate group (Scheme 1). To the best of our knowledge, this coordination mode has not been observed previously for the HSIP²⁻ ligand.^[5–7,15] One of the carboxylate groups is protonated for charge balance, as suggested by the strong absorption at 1693 cm^{-1} in the IR spectrum and strong H^+ -assisted hydrogen bonds between the free carboxylate oxygen atoms ($\text{O2A}'\cdots\text{O4}$ 2.344 and $\text{O2A}\cdots\text{O4}$ 2.436 Å, A: $x - 1/2$, $y, -z + 1/2$). As

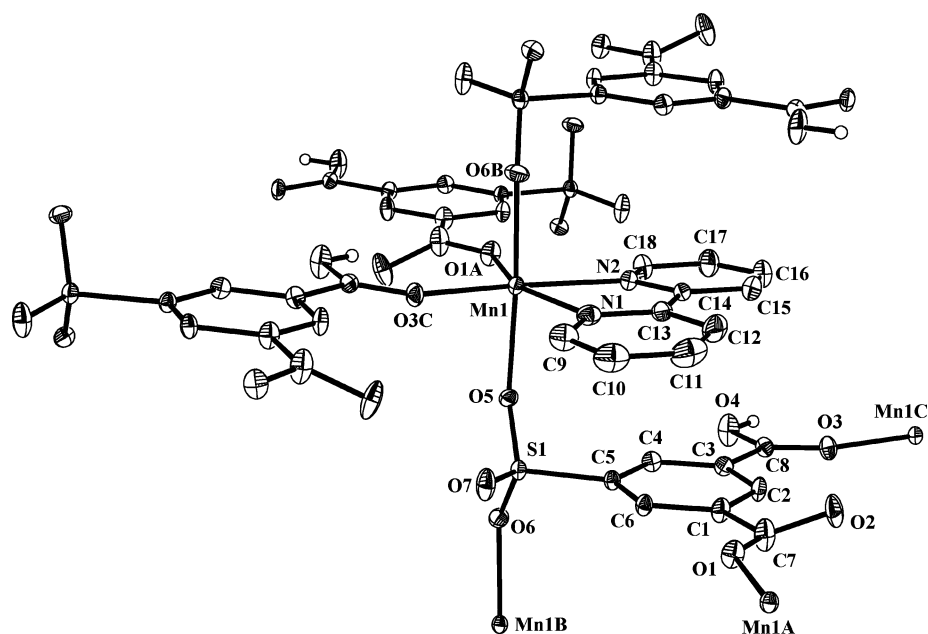


Figure 6. Molecule structure of **2** with 30% probability displacement ellipsoids.

depicted in Figure 7a, the Mn(bpy) units are connected by the carboxylate groups of HSIP²⁻ to yield almost planar 1D chains propagating along the *a* axis. The infinite chains are displaced parallel to each other so that the peripheral sulfonate oxygen atoms of each chain are able to apically bond to Mn²⁺ from the four neighboring chains to form a 3D framework, as shown in Figure 7a,b. The 3D structure features four types of rings, A–D, as depicted in Figure 7c that are characteristic of the metal–SIP compounds.^[22]

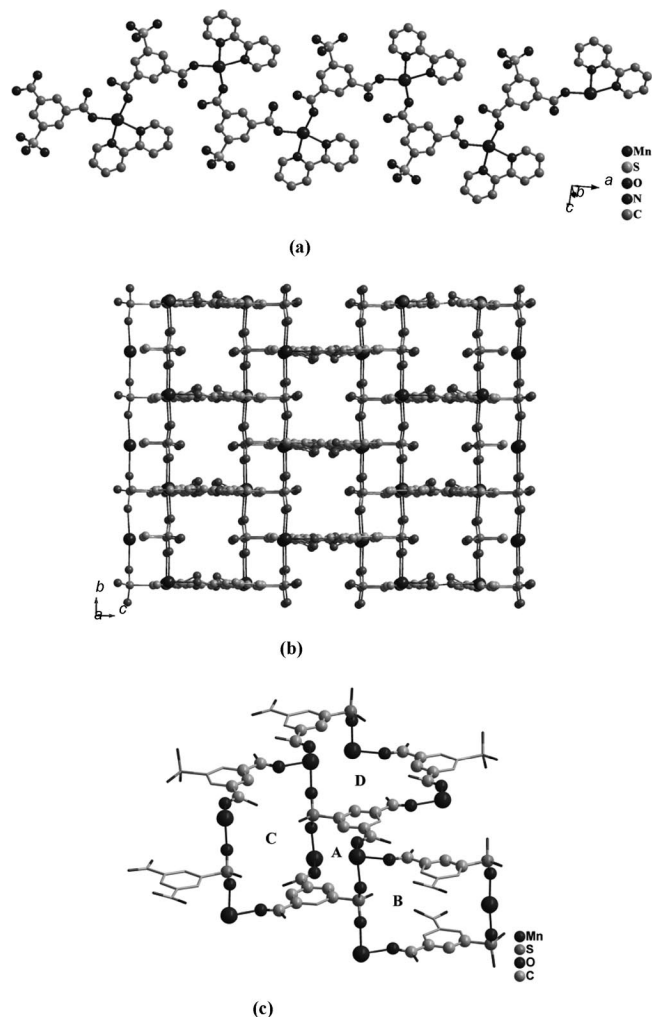


Figure 7. (a) Infinite chain formed by Mn²⁺ and the carboxylate arms; (b) 3D structure formed by interchain bonds between sulfonate oxygen atoms and Mn²⁺ at apical positions (bpy is omitted for clarity); (c) The A–D rings in the 3D framework.

Better insight into the nature of this intricate 3D framework can be achieved by the topological approach, that is, by reducing the multidimensional structures to simple node and connection nets. As depicted in Figure 8, each Mn atom is coordinated by four oxygen atoms from four HSIP²⁻ ligands and each HSIP²⁻ ligand bridges four neighboring Mn atoms (Figure 6). Therefore, the Mn atom and the HSIP²⁻ ligand both act as 4-connected nodes in a 1:1 ratio in this structure. It is interesting that the two 4-connected nodes are topologically equivalent, and the long

(Schäfli) notation is (4.6₂.6.6.6.6). Thus, the 3D structure is a binodal net with the short symbol of (4.6⁵). This type of topology, to the best of our knowledge, has never been documented for a coordination complex. A large number of potential 4-connected nets have been identified. By far the most common of these are the diamond net^[23] and to a lesser extent the CdSO₄^[24] and NbO nets.^[25] All of the 4-connected nets contain six-membered and larger rings, and examples of four-membered rings are comparatively rare in 3D coordination frameworks. Therefore, the topologic structure shown in Figure 8 presents a rare example of a 4-connected net.

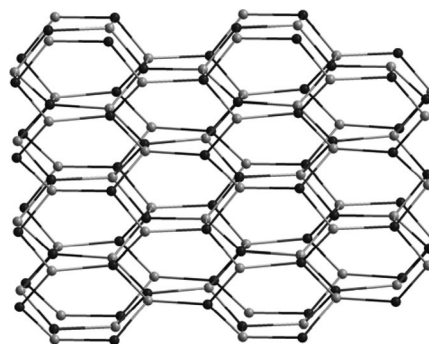


Figure 8. View of the topological net observed in **2** illustrating the 4-connected (4.6⁵) network (metal nodes are in black; ligand nodes are in gray).

Magnetic Properties

The magnetic susceptibility of **2** was recorded over 5–300 K. The plots of molar magnetic susceptibility (χ_M) and magnetic moment (μ_B) vs. temperature are shown in Figure 9. The magnetic moment per Mn²⁺ is 5.72 μ_B at 300 K, which is close to the spin-only value for the magnetically isolated high-spin Mn²⁺ (5.92 μ_B). The value remains almost constant over the temperature range 300–90 K (5.57 μ_B) and then decreases to 3.26 μ_B at 5 K. The magnetic susceptibility data between 300 and 5 K obey the Curie–Weiss law, $\chi_M = C/(T - \theta)$, where the Curie constant *C* and Weiss constant θ are 4.03 emu K mol⁻¹ and –5.79 K, respectively. The small Weiss constants in these complexes

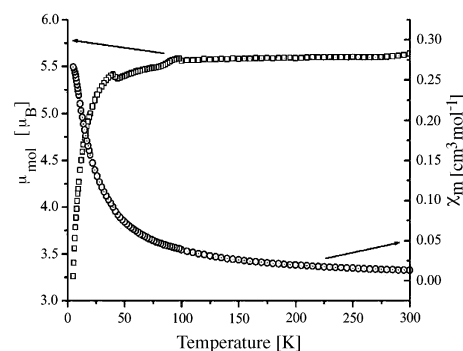


Figure 9. Plots of χ_M and magnetic moment (per mol) vs. temperature.

indicate the weak antiferromagnetic interactions between the Mn^{2+} centers, which is consistent with the slow decrease in the magnetic moment.

FTIR Spectra, Thermogravimetric Analyses, and Powder X-ray Diffraction

The FTIR spectrum of **1** shows a broad band centered at 3357 cm^{-1} , which is attributable to the O–H stretching frequency of the water cluster. This value is very close to the value of 3359 cm^{-1} in the extended water tapes.^[12] The strong absorptions at 1601 and 1563 cm^{-1} [$\nu_{\text{asym}}(\text{CO}_2)$] and 1445 cm^{-1} [$\nu_{\text{sym}}(\text{CO}_2)$] are due to the carboxylate groups. The IR spectrum of **2** shows a strong absorption at 1693 cm^{-1} , which clearly indicates the existence of a protonated carboxylate group in the structure of **2**. The strong bands at 1664 and 1443 cm^{-1} correspond to the asymmetric and symmetric stretching bands of the carboxylate groups, respectively. The absorptions in the region $1000\text{--}1200\text{ cm}^{-1}$ for the two complexes are typical for the sulfonate group. The strong absorption bands at 618 and 622 cm^{-1} for **1** and **2**, respectively, are due to $\nu_{\text{S-O}}$ stretching.

To examine the thermal stability of the two compounds and their structural variation as a function of temperature, thermogravimetric analyses (TGA) were performed on single-phase polycrystalline samples of these materials (Figure 10). The results of compound **1** show a weight loss of 14.9% in the temperature range $40\text{--}115\text{ }^\circ\text{C}$, which is due to the loss of all lattice water molecules (calcd. 14.7%). Complete decomposition was observed above $280\text{ }^\circ\text{C}$. Thermogravimetric analysis of **2** showed that the initial weight loss occurred in the temperature range $400\text{--}455\text{ }^\circ\text{C}$, which is attributable to the release of the bpy molecule (calcd. 34.3%; found 35.4%). Increasing the temperature led to the decomposition of the Mn–HSIP framework at $460\text{ }^\circ\text{C}$.

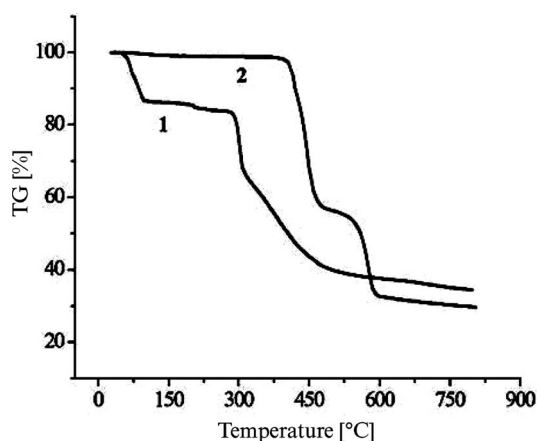


Figure 10. TG curve of compounds **1** and **2**.

Conclusions

The hydrothermal reaction system of M^{2+} –SIP, where $\text{M} = \text{Cu}$ or Mn , affords quite distinct outcomes for the two

different metals. In situ hydroxylation of SIP was observed for the first time in the case of Cu^{2+} , which produced the SIP- O^4 -bridged dicopper(II) compound $[\text{Cu}_2(\text{SIP-O})(\text{bpy})_2(\text{H}_2\text{O})_2]\cdot 7\text{H}_2\text{O}$ (**1**). The similar reaction of MnCl_2 produced the 3D coordination polymer $[\text{Mn}(\text{HSIP})(\text{bpy})]_n$ (**2**). The lattice water molecules in **1**, which form 2D-layered water with a unique 4.8^2 topology, and a discrete water octamer are alternatively located between the 2D supramolecular host sheets. Compound **2** has a 3D coordination framework with a rare 4.6^5 topology. The Mn^{2+} ions are linked by the carboxylate arms of the HSIP ligand into an infinite chain that are further pillared by the sulfonate group through apical coordination to yield a 3D architecture. This presumably provides a new strategy to build 3D frameworks based on infinite chains.

Experimental Section

General Remarks: All chemicals, including 5-sulfoisophthalic acid monosodium salt (Alfa), were purchased commercially and used without further purification. Elemental analyses were carried out with an Elementar Vario EL III analyzer, and IR spectra (KBr pellets) were recorded with a PerkinElmer Spectrum One. Thermogravimetric measurements were performed with a Netzsch STA449C apparatus under a nitrogen atmosphere with a heating rate of $10\text{ }^\circ\text{C min}^{-1}$ from 25 to $800\text{ }^\circ\text{C}$. Variable-temperature susceptibility measurements were carried out in the temperature range $5\text{--}300\text{ K}$ at a magnetic field of 0.5 T on polycrystalline samples with a Quantum Design MPMS-5 magnetometer.

$[\text{Cu}_2(\text{SIP-O})(\text{bpy})_2(\text{H}_2\text{O})_2]\cdot 7(\text{H}_2\text{O})$ (1**):** The hydrothermal reaction of fresh $\text{Cu}(\text{OH})_2$ (0.001 g , 0.1 mmol) with NaH_2SIP (0.015 g , 0.6 mmol), bpy (0.015 g , 0.1 mmol), and water (18 mL) at $165\text{ }^\circ\text{C}$ for 120 h produced green crystals of **1** (0.002 g , 5%). IR (KBr pellet): $\tilde{\nu} = 3357$ (m), 1601 (vs), 1563 (s), 1496 (m), 1476 (m), 1445 (vs), 1361 (m), 1313 (m), 1280 (m), 1285 (m), 1109 (s), 1101 (m), 1033 (s), 1101 (m), 938 (w), 815 (w), 778 (m), 731 (m), 662 (m), 618 (s) cm^{-1} . $\text{C}_{28}\text{H}_{36}\text{Cu}_2\text{N}_4\text{O}_{17}\text{S}$ (859.75): calcd. C 39.08 , H 4.19 , N 6.51 ; found C 39.03 , H 4.17 , N 6.49 .

$[\text{Mn}(\text{HSIP})(\text{bpy})]_n$ (2**):** The hydrothermal reaction of MnCl_2 (0.012 g , 0.1 mmol) with NaH_2SIP (0.026 g , 0.1 mmol), bpy (0.015 g , 0.1 mmol), triethylamine (0.1 mL), and water (18 mL) at $165\text{ }^\circ\text{C}$ for 120 h produced pale yellow crystals of **2** (0.025 g , 56%). IR (KBr pellet): $\tilde{\nu} = 3472$ (w), 3106 (w), 3083 (w), 1693 (s), 1664 (vs), 1590 (s), 1573 (s), 1471 (m), 1443 (vs), 1388 (m), 1320 (m), 1268 (s), 1154 (s), 1097 (s), 1009 (s), 907 (m), 994 (w), 761 (s), 734 (m), 669 (m), 631 (s), 622 (s), 572 (w), 551 (w) cm^{-1} . $\text{C}_{18}\text{H}_{12}\text{MnN}_2\text{O}_7\text{S}$ (455.30): calcd. C 47.48 , H 2.66 , N 6.15 ; found C 47.40 , H 2.67 , N 6.13 .

X-ray Crystallographic Studies: X-ray diffraction data of compounds **1** and **2** were collected with a Rigaku Mercury CCD diffractometer equipped with a graphite-monochromated $\text{Mo-K}\alpha$ radiation ($\lambda = 0.71073\text{ \AA}$). The CrystalClear software was used for data reduction and empirical absorption correction.^[26] The structures were solved by direct methods and successive Fourier difference syntheses and refined by the full-matrix least-squares method on F^2 (SHELXTL Version 5.1).^[27] The O2 carboxylate oxygen atom in **2** was found to be disordered over two positions. Aromatic hydrogen atoms were assigned to calculated positions with isotropic thermal parameters fixed at 1.2 times that of the attached carbon atom. Hydrogen atoms attached to water oxygen atoms were lo-

Table 3. Crystallographic data for compounds **1** and **2**.

	1	2
Empirical Formula	C ₂₈ H ₃₆ N ₄ O ₁₇ SCu ₂	C ₁₈ H ₁₂ N ₂ O ₇ SMn
Molecular mass	859.75	455.30
Temperature [K]	293(2)	293(2)
Crystal size [mm]	0.20 × 0.16 × 0.12	0.12 × 0.08 × 0.05
Crystal system	monoclinic	orthorhombic
Space group	<i>P</i> 2 ₁ / <i>c</i>	<i>Pbca</i>
<i>Z</i>	4	8
<i>a</i> [Å]	19.1828(17)	15.9207(13)
<i>b</i> [Å]	14.1577(11)	13.4252(10)
<i>c</i> [Å]	12.6442(11)	16.7567(13)
<i>α</i> [°]	90	90
<i>β</i> [°]	95.598(4)	90
<i>γ</i> [°]	90	90
<i>V</i> [Å ³]	3417.6(5)	3581.6(5)
<i>D</i> _{calcd.} [g cm ⁻³]	1.671	1.689
<i>μ</i> [mm ⁻¹]	1.389	0.901
Measured reflections	20803	20706
Independent reflections	5776	3023
Observed reflections	4661	2405
[<i>I</i> > 2σ(<i>I</i>)]		
Parameters	541	271
<i>F</i> (000)	1768	1848
Completeness [%]	99.0	98.3
2θ range [°]	5.08 to 24.71	3.14 to 25.03
Index ranges	-19 ≤ <i>h</i> ≤ 22 -16 ≤ <i>k</i> ≤ 15 13 ≤ <i>l</i> ≤ 14	-18 ≤ <i>h</i> ≤ -18 15 ≤ <i>k</i> ≤ 15 -19 ≤ <i>l</i> ≤ 19
<i>R</i> [int]	0.0530	0.0870
<i>R</i> ₁ [obsd. refl.]	0.0550	0.0659
<i>wR</i> ₂ [all refl.]	0.1249	0.0960
Largest diff. peak and hole [e Å ⁻³]	0.418/-0.331	0.616/-0.366

cated from difference maps and refined with O–H distances restrained to 0.90 Å, and isotropic thermal parameters fixed at 1.5 times that of the respective oxygen atom. The *R*₁ values are defined as $R_1 = \sum ||F_o| - |F_c|| / \sum |F_o|$ and $wR_2 = \{\sum [w(F_o^2 - F_c^2)^2] / \sum [w(F_o^2)]\}^{1/2}$. Details of the crystal parameters, data collection, and refinement are summarized in Table 3, and selected bond lengths and bond angles are listed in Table 1.

CCDC-294696 (for **1**) and -649721 (for **2**) contain the supplementary crystallographic data for this paper. These data can be obtained free of charge from The Cambridge Crystallographic Data Centre via www.ccdc.cam.ac.uk/data_request/cif.

Acknowledgments

This work was supported by the National Science Foundation of China (Grant No. 20773129 and 20473092) and 973 Program (Grant No. 2006CB932900).

[1] B. Moulton, M. J. Zaworotko, *Chem. Rev.* **2001**, *101*, 1629–1658.

- [2] O. R. Evans, R. Xiong, Z. Wang, G. K. Wong, W. Lin, *Angew. Chem.* **1999**, *111*, 557–559; *Angew. Chem. Int. Ed.* **1999**, *38*, 536–538.
- [3] M. Eddaoudi, D. B. Moler, H. L. Li, B. L. Chen, T. M. Reincke, M. O’Keeffe, O. M. Yaghi, *Acc. Chem. Res.* **2001**, *34*, 319–330.
- [4] a) C.-D. Wu, W.-B. Lin, *Angew. Chem. Int. Ed.* **2005**, *44*, 1958–1961; b) T. J. Prior, M. J. Rosseinsky, *Chem. Commun.* **2001**, 1222–1223; c) D. F. Sun, R. Cao, Y. Q. Sun, W. H. Bi, X. J. Li, Y. Q. Wang, Q. Shi, X. Li, *Inorg. Chem.* **2003**, *42*, 7512–7518.
- [5] a) A. D. Kulnych, G. K. H. Shimizu, *CrystEngComm* **2002**, *4*, 102–105; b) D.-F. Sun, R. Cao, Y.-Q. Sun, X. Li, W.-H. Bi, M.-C. Hong, Y.-J. Zhao, *Eur. J. Inorg. Chem.* **2003**, 94–98; c) A. P. Côté, G. K. H. Shimizu, *Chem. Commun.* **2001**, 251–252.
- [6] Q.-Y. Liu, L. Xu, *Eur. J. Inorg. Chem.* **2005**, 3458–3466.
- [7] Q.-Y. Liu, L. Xu, *Eur. J. Inorg. Chem.* **2006**, 1620–1628.
- [8] J. Tao, Y. Zhang, M.-L. Tong, X.-M. Chen, T. Yuen, C.-L. Lin, X.-Y. Huang, J. Li, *Chem. Commun.* **2002**, 1342–1343.
- [9] a) S. H. Gou, M. Qian, Z. Yu, C. Y. Duan, X. F. Sun, W. Huang, *J. Chem. Soc., Dalton Trans.* **2001**, 3232–3237; b) Q.-Y. Liu, L. Xu, *Cryst. Growth Des.* **2007**, *7*, 1832–1843.
- [10] S. K. Ghosh, P. K. Bharadwaj, *Inorg. Chem.* **2004**, *43*, 6887–6889.
- [11] S. Maheshwary, N. Patel, N. Sathyamurthy, A. D. Kulkarni, S. R. Gadre, *J. Chem. Phys.* **2001**, *115*, 10525–10531.
- [12] B. Q. Ma, H. L. Sun, S. Gao, *Angew. Chem. Int. Ed.* **2004**, *43*, 1374–1376.
- [13] A. F. Wells, *Structural Inorganic Chemistry*, 5th ed., Clarendon, Oxford, **1984**.
- [14] a) D. L. Long, A. J. Blake, N. R. Champness, M. Schröder, *Chem. Commun.* **2000**, 1369–1370; b) J. Fan, W.-Y. Sun, T. Okamura, W.-X. Tang, N. Ueyama, *Inorg. Chem.* **2003**, *42*, 3168–3175.
- [15] Q.-Y. Liu, L. Xu, *CrystEngComm* **2005**, *7*, 87–89.
- [16] W. B. Blanton, S. W. Gordon-Wylie, G. R. Clark, K. D. Jordan, J. T. Wood, U. Geiser, T. J. Collins, *J. Am. Chem. Soc.* **1999**, *121*, 3551–3552.
- [17] R. J. Doedens, E. Yphannes, M. I. Khan, *Chem. Commun.* **2002**, 62–63.
- [18] J. L. Atwood, L. J. Barbour, T. J. Ness, C. L. Raston, P. L. Raston, *J. Am. Chem. Soc.* **2001**, *123*, 7192–7193.
- [19] C. J. Tsai, K. D. Jordan, *J. Chem. Phys.* **1993**, *99*, 6957–6970.
- [20] B.-Q. Ma, H.-L. Sun, S. Gao, *Chem. Commun.* **2005**, 2336–2338.
- [21] C.-M. Ma, C.-N. Chen, Q.-T. Liu, D.-Z. Liao, L.-C. Li, L.-C. Sun, *New J. Chem.* **2003**, *27*, 890–894.
- [22] Z.-M. Sun, J.-G. Mao, Y.-Q. Sun, H.-Y. Zeng, A. Clearfield, *Inorg. Chem.* **2004**, *43*, 336–341.
- [23] a) L. Carlucci, G. Ciani, D. M. Proserpio, S. Rizzato, *Chem. Eur. J.* **2002**, *8*, 1519–1526; b) Y. H. Liu, H. C. Wu, H. M. Lin, W. H. Hou, K. L. Lu, *Chem. Commun.* **2003**, 60–61.
- [24] a) G. E. Kostakis, L. Casella, N. Hadjiladis, E. Monzani, N. Kourkoumelisc, J. C. Plakatouras, *Chem. Commun.* **2005**, 3859–3861; b) B. R. Bhogala, P. K. Thallapally, A. Nangia, *Cryst. Growth Des.* **2004**, *4*, 215–218.
- [25] M. Eddaoudi, J. Kim, M. O’Keeffe, O. M. Yaghi, *J. Am. Chem. Soc.* **2002**, *124*, 376–377.
- [26] *CrystalClear, version 1.3*, Rigaku Corp. **2000**.
- [27] G. M. Sheldrick, *SHELXS 97: Program for Crystal Structure Solution*, University of Göttingen, **1997**.

Received: October 23, 2007

Published Online: January 7, 2008